Clinically Relevant Doses of Methylphenidate Significantly Occupy Norepinephrine Transporters in Humans In Vivo

Jonas Hannestad, Jean-Dominique Gallezot, Beata Planeta-Wilson, Shu-Fei Lin, Wendol A. Williams, Christopher H. van Dyck, Robert T. Malison, Richard E. Carson, and Yu-Shin Ding

Background: Attention-deficit/hyperactivity disorder is a psychiatric disorder that starts in childhood. The mechanism of action of methylphenidate, the most common treatment for attention deficit hyperactivity disorder, is unclear. In vitro, the affinity of methylphenidate for the norepinephrine transporter (NET) is higher than that for the dopamine transporter (DAT). The goal of this study was to use positron emission tomography to measure the occupancy of brain norepinephrine transporter by methylphenidate in vivo in humans.

Methods: We used (S,S)-[^{11}C] methylreboxetine ([^{11}C]MRB) to determine the effective dose 50 (ED_{50}) of methylphenidate for NET. In a within-subject design, healthy subjects ($n = 11$) received oral, single-blind placebo and 2.5, 10, and 40 mg of methylphenidate 75 min before [^{11}C]MRB injection. Dynamic positron emission tomography imaging was performed for 2 hours with the High Resolution Research Tomograph. The multilinear reference tissue model with occipital cortex as the reference region was used to estimate binding potential non-displaceable (BP_{ND}) in the thalamus and other NET-rich regions.

Results: BP_{ND} was reduced by methylphenidate in a dose-dependent manner in thalamus and other NET-rich regions. The global ED_{50} was estimated to be .14 mg/kg; therefore, the average clinical maintenance dose of methylphenidate (.35–.55 mg/kg) produces 70% to 80% occupancy of NET.

Conclusions: For the first time in humans, we demonstrate that oral methylphenidate significantly occupies NET at clinically relevant doses. The ED_{50} is lower than that for DAT (.25 mg/kg), suggesting the potential relevance of NET inhibition in the therapeutic effects of methylphenidate in attention-deficit/hyperactivity disorder.

Key Words: [^{11}C]methylreboxetine, attention-deficit/hyperactivity disorder, dopamine, methylphenidate, norepinephrine transporter, positron emission tomography

The core features of attention-deficit/hyperactivity disorder (ADHD)—inattention, hyperactivity, and impulsivity—can be attributed to dysfunction in neural systems that regulate attention, executive function, motor control, and reward (1–3). The three classes of pharmacologic treatments for ADHD—psychostimulants (e.g., methylphenidate; methylphenidate [MPH]), nonstimulant catecholamine reuptake inhibitors (e.g., atomoxetine), and α2 adrenergic receptor agonists (e.g., guanfacine)—all modulate dopamine (DA) and norepinephrine (NE) neurotransmission (1,4). Small changes in extracellular NE or DA concentration affect networks of pyramidal cells in the prefrontal cortex (PFC), which regulates and sustains attention (5). The beneficial effects of DA occur at D1 receptors, whereas those of NE are believed to occur at α2 receptors (5).

The effects of MPH on the DA system have been studied extensively. Clinical doses of MPH occupy more than 50% of DAT in vivo in humans (6,7), suggesting that DA reuptake inhibition, and resultant D1 receptor activation, may be an important therapeutic mechanism in ADHD (5). The potential role of NE is supported by animal and human data (8). Consistent with the role of NE in ADHD, MPH has higher in vitro affinity for norepinephrine transporter (NET) than DAT ($K_i = 38$ vs. 193 nmol/L) (9). Low doses of MPH increase levels of NE in the PFC in animals (10), and low doses of MPH improve performance of PFC tasks in subjects with ADHD (11).

Previous positron emission tomography (PET) studies have demonstrated the specificity of MPH's active enantiomer (*d-threo*-MPH) in basal ganglia (12), and that clinical doses of MPH significantly occupy DAT (7). The absence of a suitable NET tracer has delayed similar studies of NET. The recently developed NET ligand [^{11}C]MRB has been used in NET occupancy studies of atomoxetine in humans and nonhuman primates (13–15) and to investigate NET abnormalities in cocaine dependence (16). Using this ligand, the aims of this study were 1) to measure the dose-dependent blockade of [^{11}C]MRB by MPH in the thalamus and other NET-rich regions and 2) to estimate effective dose 50 (ED_{50}), that is, the dose at which 50% of NET are occupied by MPH.

Methods and Materials

Subjects

We recruited six women and five men with no current medical problems and no psychiatric history, including ADHD. Medical and psychiatric history, review of systems, the structured interview for the DSM (17), and a physical examination were performed by a board-certified psychiatrist (JH). Laboratory tests and electrocardiogram were used to rule out any unknown medical condition. All subjects were stimulant-naive, with no history of exposure to amphetamines, cocaine, ecstasy, or MPH. Urine drug screens and pregnancy tests were negative at screening and on the morning of each scan. The study was approved by the Yale University Human Investigation Committee, and informed consent was obtained after complete description of the study to the subjects.

Magnetic Resonance Imaging

Magnetic resonance imaging (MRI) was performed on a 3T Trio (Siemens Medical Systems, Erlangen, Germany) with a circularly-

From the Department of Psychiatry (JH, WAW, CHvD, RTD) and Department of Diagnostic Radiology (J-DG, BP-W, S-FL, REC, Y-SD), Yale PET Center, Yale University School of Medicine, New Haven, Connecticut.

Address correspondence to Yu-Shin Ding, Ph.D., P.O. Box 208048, New Haven, CT 06520-8048; E-mail: yu-shin.ding@yale.edu.

Received Mar 4, 2010; revised Jun 14, 2010; accepted Jun 17, 2010.

0006-3223/$36.00
doi:10.1016/j.biopsych.2010.06.017

polarized head coil. MR acquisition was a Sag three-dimensional magnetization-prepared rapid gradient-echo sequence with 3.34-msec echo time, 2500-msec repetition time, 1100-msec inversion time, 7° flip angle, and 180 Hz/pixel bandwidth. The image dimensions were 256 × 256 × 176, and pixel size was .98 × .98 × 1.0 mm.

MPH Administration

In nonhuman primates, MPH reaches peak concentrations in the brain by 60 min (7). We conducted a preliminary duration study in two human subjects to determine how much time it takes from oral MPH administration to maximum occupancy of brain NET. Because peak displacement of [^{11}C]MRB by MPH was achieved by 75 min (Supplement 1), we chose 75 min as the time between oral MPH dosing and [^{11}C]MRB injection for this occupancy study. Each subject had four PET scans on three different days, separated by at least 1 week. On the first day, subjects received placebo before the morning scan and MPH 2.5 mg before the afternoon scan. On the second and third study days, they received MPH 10 and 40 mg, respectively. Study medication was prepared by the Yale–New Haven Hospital Pharmacy and administered 76 ± 12 min before each [^{11}C]MRB injection. Subjects were only told that they would receive either placebo or MPH. Blood samples for determination of plasma levels of MPH were obtained at the beginning and end of each PET scan (~ 75 and ~ 195 min after MPH administration). Plasma levels of *d-threo*-MPH were determined with capillary gas chromatography-mass spectrometry.

PET Imaging

[^{11}C]MRB was synthesized as described previously (18), and PET images were acquired using the High Resolution Research Tomograph (HRRT; Siemens/CTI, Knoxville, Tennessee) with a reconstructed image resolution of approximately 3 mm. Following a transmission scan, [^{11}C]MRB was injected intravenously as a 1-min bolus by an infusion pump. List-mode data were acquired for 120 min. Head motion correction was performed using an optical tracking tool (Vicra, NDI Systems, Waterloo, Canada) and a rigid tool attached to a swim cap.

Arterial Input Function Measurement

Radial artery blood samples were obtained on Days 1 and 3 to measure the arterial input function for the purpose of kinetic modeling (Supplement 1).

Image Reconstruction and Motion Correction

Dynamic scan data were reconstructed with corrections for attenuation, normalization, scatter, randoms, dead time, and motion using the MOLAR algorithm (motion-compensation ordered subset-expectation maximization list-mode algorithm for resolution-recovery reconstruction) (19) with the following frame timing: 6 × 30 sec; 3 × 1 min; 2 × 2 min; 22 × 5 min. A second step of motion correction was performed after reconstruction by realigning each frame to an early summed image (0–10 min postinjection) using a six-parameter mutual information algorithm (FMRIB's Linear Image Registration Tool, FMRIB's Software Library 3.2, Analysis Group, Oxford University Centre for Functional Magnetic Resonance Imaging of the Brain, Oxford, United Kingdom).

Delineation of Regions of Interest

A summed image (0–10 min) was generated and used for coregistration to the subject's MRI. The MRI was then coregistered to the template MRI to determine regions of interest (ROIs). Cortical regions, thalamus, basal ganglia, and hypothalamus were identified with the Automated Anatomical Labeling template (20). Additional ROIs were delineated on the template MRI, including thalamic subnuclei, locus ceruleus (LC), pontine and midbrain raphe nuclei, and red nucleus. The volume and location of ROIs were determined based on the Talairach atlas as previously described (16).

Image Analysis

Parametric images of [^{11}C]MRB volume of distribution (V_T) and binding potential non-displaceable (BP_{ND}) (21) values were calculated using the multilinear reference tissue models Multilinear Analysis 1 (MA1) (22) and Multilinear Reference Tissue Model 2 (MRTM2) (23) (Supplement 1). The occipital cortex was selected as the reference region because postmortem studies in humans have shown that this region has lower levels of NET than the striatum (24).

Determination of ED_{50} for MPH

ED_{50} is the dose in mg/kg body weight at which 50% of brain NET are occupied. The MPH ED_{50} was estimated by fitting the MRTM2 BP_{ND} values as a function of the MPH dose (D_{MPH}) using Equation 1:

$$BP_{\mathrm{ND}}^{\mathrm{MRTM2}} = BP_{\mathrm{ND}}^{\infty} + \frac{BP_{\mathrm{ND}}^{0} - BP_{\mathrm{ND}}^{\infty}}{1 + \dfrac{D_{\mathrm{MPH}}}{ED_{50}}}$$

Where BP_{ND}^{0} represents [^{11}C]MRB MRTM2 BP_{ND} at baseline, BP_{ND}^{∞} represents [^{11}C]MRB remaining MRTM2 BP_{ND} at saturation, and D_{MPH} represents dose of MPH. Equation 1 allows for different levels of nondisplaceable binding between regions. If [^{11}C]MRB nondisplaceable binding in the reference and target regions are the same, then BP_{ND}^{∞} would equal zero, and BP_{ND}^{0} would equal the true BP_{ND} value for [^{11}C]MRB. Conversely, if nondisplaceable binding levels are different, then BP_{ND}^{∞} would equal the relative difference of the nondisplaceable volumes (V_{ND}) in the target and reference regions, as shown in Equation 2:

$$BP_{\mathrm{ND}}^{\infty} = \frac{V_{\mathrm{ND}}^{\mathrm{Target}} - V_{\mathrm{ND}}^{\mathrm{Reference}}}{V_{\mathrm{ND}}^{\mathrm{Reference}}}$$

The true baseline BP_{ND} can also be computed from BP_{ND}^{0} and BP_{ND}^{∞} as:

$$BP_{\mathrm{ND}} = \frac{BP_{\mathrm{ND}}^{0} - BP_{\mathrm{ND}}^{\infty}}{1 + BP_{\mathrm{ND}}^{\infty}}$$

To test whether the nondisplaceable binding is different between the reference region and some of the target regions, two sets of fits were performed, with or without the assumption that BP_{ND}^{∞} is equal to zero, and compared using the *F* test. To test whether the ED_{50} estimates were significantly different across regions, the total sum of squares from all regional fits was compared with the sum of squares of a coupled fit across all regions using a global ED_{50} estimate also using the *F* test. The MPH IC_{50}, that is, the plasma concentration at which 50% of NET are occupied, was estimated as $IC_{50} = \alpha \times ED_{50}$, where α is the slope of the regression line linking the plasma concentration of *d-threo*-MPH to the dose of MPH.

Statistical Analysis

The data were first examined using descriptive statistics. In the primary analysis, repeated-measures analysis of variance (ANOVA) was used to assess the effect of MPH dose (placebo, 2.5, 10, and 40 mg) on BP_{ND} in the thalamus, which was chosen as the primary end point because it is the largest NET-rich region. Then, exploratory analyses were conducted for all individual ROIs. Post hoc pair-

Table 1. Radiotracer ([^{11}C]MRB) Characteristics

MRB / [^{11}C]MRB — MPH	Methylphenidate 0 mg	2.5 mg	10 mg	40 mg	
Injected Dose (mCi)	17.8 ± 4.1	15.9 ± 4.1	15.8 ± 3.9	17 ± 3.9	All p values > .2[a]
Injected Mass (nmoles)	1.7 ± .9	1.5 ± .7	2 ± .6	1.5 ± .6	All p values > .3
Free Fraction	.13 ± .03	.12 ± .02	.12 ± .02	.12 ± .02	All p values > .5

[^{11}C]MRB, (S,S)-[^{11}C] methylreboxetine.
[a]Pairwise comparisons between each of the four doses all had $ps > .2$.

wise analyses were performed to examine differences between individual MPH doses. A p value $< .05$ was considered statistically significant.

Results

Demographic and Radiotracer Characteristics

The mean age was 34 ± 8 years, and the mean body mass index was 28 ± 5 kg/m^2. Radiotracer characteristics are summarized in Table 1. MPH was well tolerated, and only one subject experienced transient anxiety after the 40-mg dose. The 75- and 195-min plasma levels of the active enantiomer *d-threo*-MPH were 1.5 ± 1.2 and .6 ± .4 ng/mL (2.5 mg), 3.1 ± 3 and 2.8 ± 1.7 ng/mL (10 mg), and 22.9 ± 13.9 and 15 ± 4.4 ng/mL (40 mg), respectively. For correlation between plasma levels of *d-threo*-MPH and MPH dose (mg/kg), please refer to Supplement 1. The doses of MPH (in mg/kg) were used as covariates to analyze the binding of [^{11}C]MRB.

Effect of MPH on [^{11}C]MRB V_T in Occipital Cortex

The arterial input function was measured during the placebo and 40-mg scans in nine subjects to assess the effect of MPH on the distribution volume of the reference region (occipital cortex) from MA1 (Supplement 1, Equation 1). In the occipital cortex, [^{11}C]MRB V_T was 4.2 ± .9 ml/cm^3 at baseline and 3.8 ± 1.0 ml/cm^3 after 40 mg MPH (relative difference = –9% ± 17%; $p = .13$, paired Student's t test, $n = 9$). The [^{11}C]MRB plasma free fraction (f_p) was 13% ± 3% at baseline and 12% ± 2% after 40 mg (relative difference = –3% ± 15%; $p = .40$, paired Student's t test, $n = 9$). Consequently, the [^{11}C]MRB normalized distribution volumes (V_T/f_p) in the occipital cortex were 34 ± 5 ml/cm^3 at baseline and 32 ± 4 ml/cm^3 after 40 mg. The small relative difference (–5 ± 15%; $p = .27$, paired Student's t test, $n = 9$) suggests that MPH did not displace [^{11}C]MRB binding in the occipital cortex (Figure 1A), thus supporting its use as the reference region. As a comparison, in other NET-poor regions such as the putamen and the caudate, V_T/f_P at baseline was 33 ± 5 mL and 26 ± 4 mL, respectively, and the V_T/f_P difference between baseline and 40 mg MPH was 2% ± 16% and 4% ± 17%, respectively. A similar ED_{50} estimate was obtained when the putamen was used as a reference region (see Supplement 1 for details).

Correlation Between [^{11}C]MRB BP_{ND} Estimated with MA1 and MRTM2

The BP_{ND} estimated for all NET-rich regions with MA1 and MRTM2 were highly correlated ($y = .909, x + .078, r^2 = .821$, where x represents the MA1 BP_{ND} values and y represents the MRTM2 BP_{ND} values; Figure 1B). Because MA1 values were only available for scans with arterial samples, subsequent analyses were performed with MRTM2 to use all the acquired scans.

Dose-Dependent Displacement of [^{11}C]MRB by MPH

There was a dose-dependent reduction of [^{11}C]MRB BP_{ND} by MPH in all NET-rich regions (Figures 2 and 3). In the thalamus, BP_{ND} at baseline was .52 ± .12, and this decreased to .44 ± .14 after 2.5 mg, to .34 ± .08 after 10 mg, and to .26 ± .06 after 40 mg. Repeated-measures ANOVA showed a highly significant main effect of MPH dose on BP_{ND} [$F(3,27) = 29, p < .0001$]. Post hoc pairwise comparisons demonstrated statistically significant differences in BP_{ND} in the thalamus for each MPH dose increment, that is, 0 versus 2.5 mg [$F(1,10) = 12.3, p = .006$], 2.5 versus 10 mg [$F(1,10) = 9.8, p = .011$], and 10 versus 40 mg [$F(1,9) = 34.3, p < .0001$]. This demonstrates that each of the three dose increments caused statistically significant displacement of [^{11}C]MRB.

NET Occupancy: ED_{50} and IC_{50}

As can be seen in Figure 3, the reduction of MRTM2 BP_{ND} estimates in regions such as LC, raphe nuclei, and hypothalamus ex-

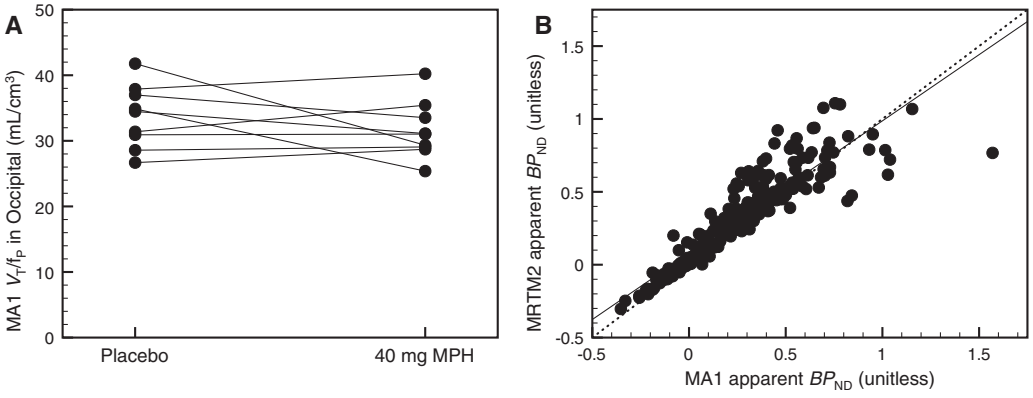

Figure 1. (A) In the reference region (occipital cortex), the (S,S)-[^{11}C] methylreboxetine ([^{11}C]MRB) normalized distribution volumes (V_T/f_P) were 34 ± 5 mL/cm^3 at baseline and 32 ± 4 mL/cm^3 after 40 mg. The small relative difference (–5 ± 15%) suggests that methylphenidate (MPH) did not displace [^{11}C]MRB binding in the occipital cortex. **(B)** The binding potential non-displaceable (BP_{ND}) estimated with Multilinear Analysis 1 (MA1) and Multilinear Reference Tissue Model 2 (MRTM2) were highly correlated: $y = .909, x + .078, r^2 = .821$, where x represents the MA1 BP_{ND} values and y represents the MRTM2 BP_{ND} values.

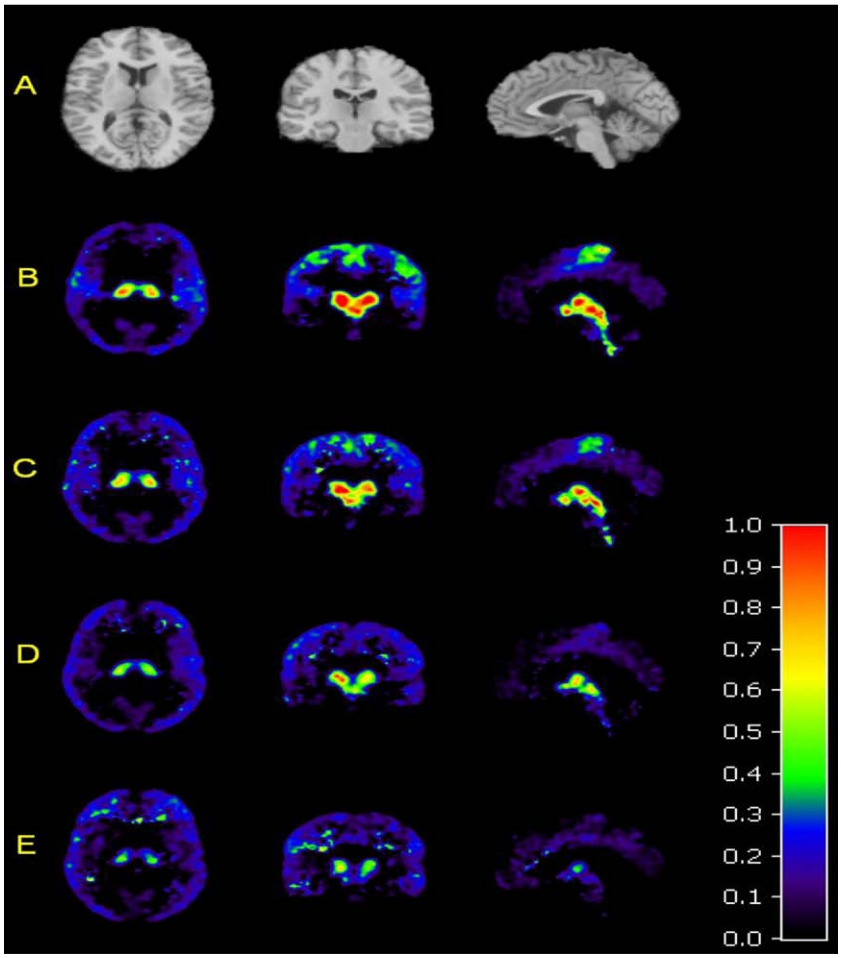

Figure 2. Template magnetic resonance imaging and average positron emission tomography images ($n = 11$) showing (S,S)-[^{11}C] methylreboxetine binding after administration of methylphenidate (MPH) 0, 2.5, 10, and 40 mg. **(A)** Axial, coronal, and sagittal views of the template magnetic resonance image used to determine regions of interest. **(B)** Axial, coronal, and sagittal views of the average positron emission tomography image of mean (S,S)-[^{11}C] methylreboxetine binding at baseline, and **(C)** after MPH 2.5 mg, **(D)** 10 mg, and **(E)** 40 mg. The color scale denotes binding potential.

ceeded 80% at 40 mg, whereas in the thalamus and thalamic subnuclei, displacement was 50% to 60%. These regional differences in the reduction of MRTM2 BP_{ND} estimates could be due to a higher ED_{50} or higher nonspecific binding in the thalamus. Assuming that nonspecific binding in a region of interest is different from that in the reference region, MPH ED_{50} and NET occupancy can be estimated with three-parameter fits (BP^{0}_{ND}, ED_{50},BP^{∞}_{ND}) using Equation 1. Assuming that nonspecific binding in a region of interest is the same as in the reference region (i.e., $BP^{\infty}_{ND} = 0$) MPH ED_{50} and NET occupancy can be estimated with two-parameter fits (BP^{0}_{ND}, ED_{50}).

In the thalamus, the assumption of nonuniform nonspecific binding led to significantly better fits [$F(1,37) = 4.2$, $p < .05$; Figure 4A and 4B]. Using the two-parameter fit, ED_{50} would have been estimated to be .42 ± .13 mg/kg (Figure 4A), whereas it was estimated to be .08 ± .06 mg/kg using the three-parameter fit (Figure 4B). BP^{0}_{ND} and BP^{∞}_{ND} were estimated to be .52 ± .03 and .21 ± .06, respectively, and [^{11}C]MRB true BP_{ND} was estimated to be .25 ± 07 (using Equation 3). NET occupancy at 40 mg would have been estimated to be 48% using the two-parameter fit (Figure 4A) and 85% using the three-parameter fit (Figure 4B). Conversely, in nonthalamic regions the two-fit model led to statistically better fits (all F values $< .63$, all p values $> .43$; Figure 4C). Comparing individual fits in the six main regions of interest (i.e., including the thalamus but excluding its subnuclei) and coupled fits with a common ED_{50} for all

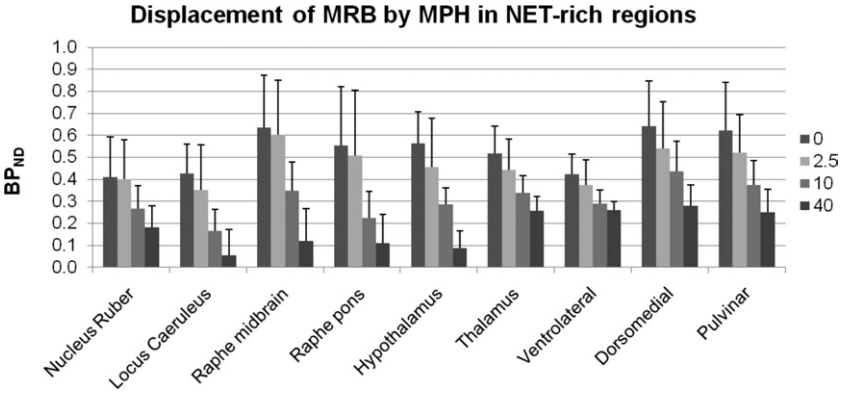

Figure 3. Dose-dependent displacement of (S,S)-[^{11}C] methylreboxetine binding ([^{11}C]MRB) by methylphenidate (MPH) in norepinephrine transporter (NET)-rich regions. Each cluster of bar graphs denotes, from left to right, mean binding potential non-displaceable (BP_{ND}) at baseline (dark gray), after MPH 2.5 mg (light gray), 10 mg (gray), and 40 mg (black). Error bars denote standard deviation.

six regions, the ED_{50} estimates are not statistically different across regions [$F(5,227) = .95$, $p = .45$; for these fits, BP^{0}_{ND} was fixed to zero in all regions except the thalamus]. In conclusion, the regional differences in maximum displacement are most consistent with higher nonspecific binding in the thalamus. Using data from all NET-rich regions, the global ED_{50} estimate was .14 ± .02 mg/kg.

The IC_{50} is the plasma concentration of *d-threo*-MPH at which 50% of NET in the brain are occupied. Assuming a linear relationship between dose (mg/kg) and plasma level, and using the global ED_{50} estimate and the regression line in Figure S1 in Supplement 1, the IC_{50} of MPH was estimated to be 4.7 ng/mL.

Discussion

MPH Occupancy of NET

This is the first in vivo study in humans showing that clinically relevant doses of MPH occupy significant levels of NET. Although MPH has been used for the treatment of ADHD for decades, the exact mechanism of action is unclear. Stimulants enhance synaptic concentrations of DA and NE, *d*-amphetamine by increasing catecholamine release, and MPH by inhibiting catecholamine reuptake. Currently, it is believed that MPH's therapeutic effects in ADHD are due mostly to its DAT inhibition; however, here we show that MPH also binds to NET with high affinity. The global ED_{50} of MPH was estimated to be .14 mg/kg. Because occupancy equals dose/(dose + ED_{50}), an MPH dose of .5 mg/kg would produce approximately 80% NET occupancy. This is consistent with clinical dosing. The average efficacious maintenance dose of MPH is .7–.9 mg/kg/day in children (25) and 1.1 mg/kg/day in adults (26). Because of its short half-life, immediate-release formulations of MPH are given twice daily, so that a total daily dose of .7–1.1 mg/kg corresponds to .35–.55 mg/kg per dose. Therefore, the average efficacious maintenance doses of MPH used in children and adults occupy 70% to 80% of NET but only 60% to 70% of DAT, based on the estimated ED_{50} value of .14 mg/kg for NET determined in this study and the value of .25 mg/kg for DAT determined previously (7). The efficacy threshold varies for medications that target receptors and transporters in the brain. For instance, antidepressants that block the serotonin transporter require 80% blockade (27), whereas antipsychotics only require 60% to 70% blockade of dopamine D2 receptors (28). The degree of NET and DAT occupancy that is required for the therapeutic effects of MPH in ADHD remains to be determined. Studies showing that therapeutic doses of MPH caused only 70% DAT occupancy (6,7) assumed that all of MPH's therapeutic effects occur by blocking DAT. However, this assumption may not be true because there is another possibility—that is, the therapeutic efficacy occurred at doses that blocked only 70% of DAT, not because 70% DAT blocking was sufficient or necessary for therapeutic efficacy but because at that same dose over 80% of NET was blocked. That is the hypothesis that emerged from our data and that has yet to be proven. However, studies showing MPH efficacy at 70% DAT occupancy do not disprove our hypothesis, or prove that 70% DAT occupancy is necessary and sufficient to produce the therapeutic effects of MPH seen in ADHD.

In summary, our results suggest that the therapeutic effects of MPH in ADHD may be mediated through NET inhibition, in addition to DAT inhibition.

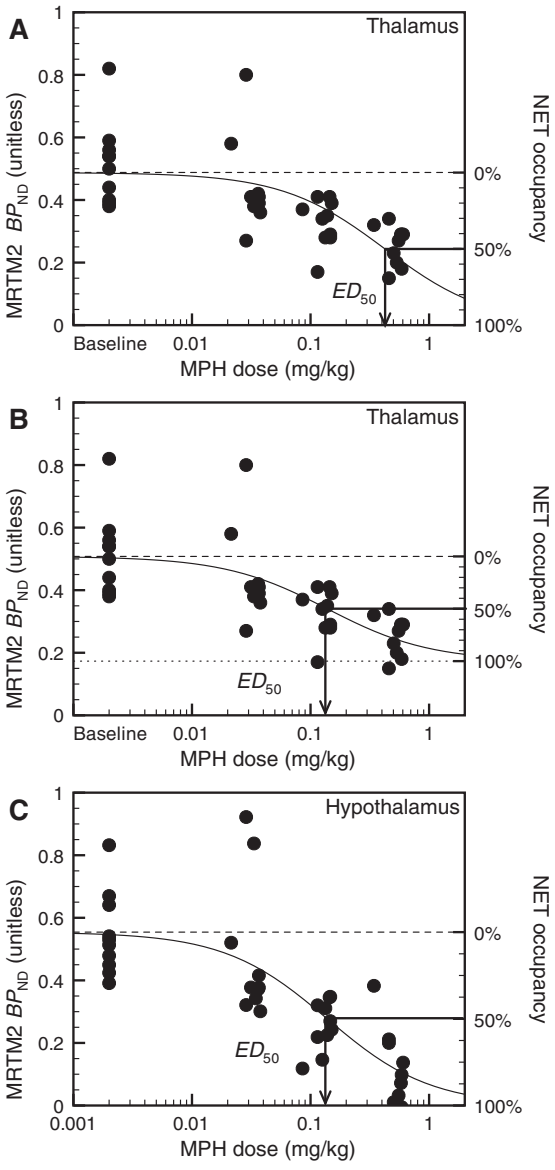

Figure 4. Dose–response curve in the thalamus **(A and B)** and the hypothalamus **(C)**. **(A)** Two-parameter fit (i.e., binding potential non-displaceable, BP^{∞}_{ND}, is assumed to be equal to zero) in the thalamus; the solid line corresponds to the line of best fit, and the dashed line corresponds to the Multilinear Reference Tissue Model 2 (MRTM2) BP_{ND} value at baseline on the left y axis or 0% occupancy on the right y axis; in this case, 100% occupancy corresponds to BP_{ND} equal to zero. **(B)** Three-parameter (i.e., BP^{0}_{ND}, IC_{50}, and BP^{∞}_{ND}) fit in the thalamus; the solid line corresponds to the line of best fit, the dotted line correspond to the MRTM2 BP_{ND} value at saturation (i.e., BP^{∞}_{ND}) on the left y axis or 100% occupancy on the right y axis, and the dashed line corresponds to the MRTM2 BP_{ND} value at baseline (i.e., BP^{0}_{ND}) on the left y axis or 0% occupancy on the right y axis. **(C)** Dose–response curve in the hypothalamus and two-parameter fit. In the thalamus, the three-parameter model produces a significantly better fit [$F(1,37) = 4.2$, $p < .05$]. In all other norepinephrine transporter (NET)-rich regions, including the hypothalamus, the two-parameter model is more suitable [all $F(1,37)$ values $< .63$ and all p values $> .43$]. The two-parameter model in the thalamus **(A)** produces a higher effective dose 50 (ED_{50}) estimate (.42 mg/kg) and lower occupancy estimates (shown on the left y axis) than the three-parameter model in the thalamus **(B)** and the two-parameter model in nonthalamic regions **(C)**. Fits shown in B and C share a common ED_{50} parameter (.14 mg/kg) because there is no significant difference between ED_{50} estimates in the various regions of interest [$F(5,227) = .95$, $p = .45$], when using the three-parameter model in the thalamus and the two-parameter model elsewhere. MPH, methylphenidate.

NET and DAT, NE and DA

Interestingly, NET has greater affinity for DA than for NE (29), and whether DAT or NET is the predominant protein clearing DA depends on the abundance of the two transporters in a given region (30). Studies in rats showed that administration of MPH (.5 mg/kg, intraperitoneal) produced a maximal increase in NE levels substantially larger than the increase in DA in the prefrontal cortex (10). In contrast, MPH (.75 mg/kg, oral) produced a similar DA and NE content in the frontal cortex of mice with a significant increase in DA content, whereas no significant change was observed in NE levels compared with the saline-administered controls (31). Because the ED_{50} estimate of MPH for NET (.14 mg/kg) from our study in humans is lower than that for DAT (.25 mg/kg), it is possible that lower doses of MPH inhibit dopamine reuptake by blocking NET rather than DAT. Medications such as atomoxetine could actually exert their therapeutic effects through DA reuptake inhibition even though they are "norepinephrine reuptake inhibitors." That is, even though atomoxetine blocks only NET and not DAT, its therapeutic effects could be due to DA reuptake inhibition because NET in the PFC may be required for DA reuptake.

Heterogeneous Nonspecific Binding

Consistent with the known distribution of NET, we found the highest levels of [^{11}C]MRB binding in the LC, thalamus, and some midbrain nuclei, and the lowest binding in occipital cortex and striatum (24,32). As described earlier, in the thalamus, 40 mg of MPH displaced only 50% to 60% of [^{11}C]MRB compared with more than 80% in other regions. The most likely explanation for this is higher nonspecific binding in the thalamus, which has been described with other NET ligands. Other explanations seem less likely. Although [^{11}C]MRB has some affinity for the serotonin transporter (IC_{50} = 310 nmol/L), if binding to the serotonin transporter prevented complete displacement in the thalamus, one would expect to see a similar effect in the raphe nuclei. This was not the case. In our previous occupancy study in humans, high doses of atomoxetine (100 mg) were unable to displace [^{11}C]MRB completely in the thalamus (33). We therefore conclude that in humans, the thalamus has higher nonspecific binding for [^{11}C]MRB, which is consistent with the heterogeneous nonspecific binding of earlier NET ligands (34,35). Some regional variation in the level of nondisplaceable binding occurs with most ligands due to a number of factors, including regional variation in the percentages of gray and white matter. To detect such regional variation requires two conditions: 1) that the ligand intrinsically has a low BP_{ND} value, so that nonspecific binding is a significant fraction of the total baseline tracer binding and 2) that a blocking study is performed that approaches or reaches 100% blockade. Thus, we believe that regional variation in nonspecific binding on the order of that found here is most likely common, and that this [^{11}C]MRB study is ideally suited to detect such variation.

Choice of Reference Region

NET are present in most brain regions and, with the exception of LC, the density of NET as measured by autoradiography in humans is not in great contrast across regions (24). The lowest density of NET was found in the occipital cortex, followed by the caudate and putamen, and these regions have been investigated as reference regions (33). In this study, no significant change of V_T or V_T /f_P was found in these three regions between the placebo and 40-mg MPH conditions, and the putamen and occipital had similar V_T values. The fact that the occipital cortex has lower levels of NET than the striatum (24) and that it is a relatively bigger region with a simpler shape than the caudate and putamen makes it more suitable as the reference region for this study, especially when ROIs are delineated with an automated template. Using the putamen as a reference region would have lead to similar or slightly lower ED_{50} estimates (Supplement 1), which would have resulted in similar or slightly overestimated occupancy of NET by MPH.

Role of Prefrontal Cortex and Other Regions in ADHD

It is hypothesized that therapeutic effects of medications used for ADHD occur mostly in the PFC (5). Studies also suggested that effects on delayed responding and working memory are mediated by noradrenergic afferents from LC (the highest NET density region) to PFC (8,36). Although the density of NET in PFC is too low to detect changes in occupancy with PET, it is important to point out that two neocortical regions, paracentral lobule and the supplementary motor area, have a NET density high enough to detect displacement of [^{11}C]MRB by MPH (Supplement 1). These two regions are in fact involved in the response to MPH and inhibition control during cognitive tasks, respectively (37,38). Although we cannot assess the effect of MPH in the PFC directly, our assumption is that the global ED_{50} calculated using NET-rich regions, including the neocortical paracentral lobule, is similar to the ED_{50} in regions with lower NET density, such as the PFC. Occupancy depends on the free drug level in the tissue, which depends on the free drug level in the plasma and will thus be the same throughout the brain. Importantly, we demonstrated that MPH occupied NET in regions that have been implicated in ADHD, such as the LC, which maintains alerting/vigilance; the thalamus and brain stem, which help module attention and filter interfering stimuli; and the thalamic pulvinar nucleus, which is involved in orienting to a stimulus (2) and which may be smaller in ADHD (39).

Conclusions

We have shown that MPH at clinically relevant doses blocks 70% to 80% of NET, whereas previous studies estimated that MPH blocks only 60% to 70% of DAT at similar doses. Therefore, NET blockade may be important in the therapeutic effects of MPH in ADHD. Whether there is an underlying abnormality in DAT, NET, the α2 adrenergic receptor, or the dopamine D1 receptor, in ADHD is not known (5). It was initially thought that DAT density was lower in ADHD; however, this has since been refuted (6). It remains to be determined whether there is an inherent difference in NET density in stimulant-naive subjects with ADHD, and this study is currently under way.

We thank the staff members of the Yale University Positron Emission Tomography Center for their technical expertise and support, the staff members at the Yale Cognitive Disorders Clinic for their help in recruiting and screening subjects, Tom Cooper at Nathan S. Kline Institute for Psychiatric Research (Orangeburg, New York) for measuring blood levels of methylphenidate, and the individuals who volunteered for this study. Support for this study was provided by the National Institute on Drug Abuse (Grant Nos. DA019062, R56DA19062). JH was supported by Grant No. UL1 RR024139 (Clinical Translational Science Awards) from the National Center for Research Resources, a component of the National Institutes of Health, and National Institutes of Health roadmap for Medical Research, and from Grant No. K12 DA000167.

Christopher H. van Dyck's spouse and Yale University have a license agreement with Shire Pharmaceuticals for the development of Intuniv (guanfacine) for the treatment of attention-deficit/hyperactivity disorder and related disorders. None of the other authors reported any biomedical financial interests or potential conflicts of interests.

Supplementary material cited in this article is available online.

1. Makris N, Biederman J, Monuteaux MC, Seidman LJ (2009): Towards conceptualizing a neural systems-based anatomy of attention-deficit/hyperactivity disorder. *Dev Neurosci* 31:36–49.
2. Bush G (2010): Attention-deficit/hyperactivity disorder and attention networks. *Neuropsychopharmacology* 35:278–300.
3. Dickstein SG, Bannon K, Castellanos FX, Milham MP (2006): The neural correlates of attention deficit hyperactivity disorder: An ALE meta-analysis. *J Child Psychol Psychiatry* 47:1051–1062.
4. Madras BK, Miller GM, Fischman AJ (2005): The dopamine transporter and attention-deficit/hyperactivity disorder. *Biol Psychiatry* 57:1397–1409.
5. Arnsten AF (2009): Toward a new understanding of attention-deficit hyperactivity disorder pathophysiology: An important role for prefrontal cortex dysfunction. *CNS Drugs* 23(suppl 1):33–41.
6. Swanson JM, Volkow ND (2009): Psychopharmacology: Concepts and opinions about the use of stimulant medications. *J Child Psychol Psychiatry* 50:180–193.
7. Volkow ND, Wang GJ, Fowler JS, Gatley SJ, Logan J, Ding YS, *et al.* (1998): Dopamine transporter occupancies in the human brain induced by therapeutic doses of oral methylphenidate. *Am J Psychiatry* 155:1325–1331.
8. Biederman J, Melmed RD, Patel A, McBurnett K, Konow J, Lyne A, *et al.* (2008): A randomized, double-blind, placebo-controlled study of guanfacine extended release in children and adolescents with attention-deficit/hyperactivity disorder. *Pediatrics* 121:e73–e84.
9. Eshleman AJ, Carmolli M, Cumbay M, Martens CR, Neve KA, Janowsky A (1999): Characteristics of drug interactions with recombinant biogenic amine transporters expressed in the same cell type. *J Pharmacol Exp Ther* 289:877–885.
10. Berridge CW, Devilbiss DM, Andrzejewski ME, Arnsten AF, Kelley AE, Schmeichel B, *et al.* (2006): Methylphenidate preferentially increases catecholamine neurotransmission within the prefrontal cortex at low doses that enhance cognitive function. *Biol Psychiatry* 60:1111–1120.
11. Aron AR, Dowson JH, Sahakian BJ, Robbins TW (2003): Methylphenidate improves response inhibition in adults with attention-deficit/hyperactivity disorder. *Biol Psychiatry* 54:1465–1468.
12. Ding YS, Fowler JS, Volkow ND, Dewey SL, Wang GJ, Logan J, *et al.* (1997): Chiral drugs: Comparison of the pharmacokinetics of [^{11}C]d-*threo* and *L-threo*-methylphenidate in the human and baboon brain. *Psychopharmacology* 131:71–78.
13. Logan J, Wang GJ, Telang F, Fowler JS, Alexoff D, Zabroski J, *et al.* (2007): Imaging the norepinephrine transporter in humans with (S,S)-[^{11}C]O-methyl reboxetine and PET: Problems and progress. *Nucl Med Biol* 34:667–679.
14. Ding YS, Naganawa M (2009): Clinical doses of atomoxetine significantly occupy both norepinephrine and serotonin transporters: Implications on treatment of depression and ADHD. *J Nucl Med* 50(suppl 2):127P.
15. Gallezot JD, Weinzimmer D (2008): Evaluation of [C 11]MRB for receptor occupancy studies of norepinephrine transporters. *Neuroimage* 41:T49.
16. Ding YS, Singhal T, Planeta-Wilson B, Gallezot JD, Nabulsi N, Labaree D, *et al.* (2010): PET imaging of the effects of age and cocaine on the norepinephrine transporter in the human brain using (S,S)-[^{11}C]O-methylreboxetine and HRRT. *Synapse* 64:30–38.
17. American Psychiatric Association (2000): *Diagnostic and Statistical Manual of Mental Disorders*, *4th* ed., text revision. Washington, DC: American Psychiatric Press.
18. Ding YS, Lin KS, Garza V, Carter P, Alexoff D, Logan J, *et al.* (2003): Evaluation of a new norepinephrine transporter PET ligand in baboons, both in brain and peripheral organs. *Synapse* 50:345–352.
19. Carson RE, Barker WC, Liow JS, Adler S, Johnson CA (2003): Design of a motion-compensation OSEM list-mode algorithm for resolution-recovery reconstruction of the HRRT. *Conference Record of the IEEE Nuclear Science Symposium and Medical Imaging Conference M16-6*. Nuclear Science Symposium Conference Record, IEEE 5:3281–3285. http://ieeexplore.ieee.org/xpls/abs_all.jsp?arnumber=1352597.
20. Tzourio-Mazoyer N, Landeau B, Papathanassiou D, Crivello F, Etard O, Delcroix N, *et al.* (2002): Automated anatomical labeling of activations in SPM using a macroscopic anatomical parcellation of the MNI MRI single-subject brain. *Neuroimage* 15:273–289.
21. Innis RB, Cunningham VJ, Delforge J, Fujita M, Gjedde A, Gunn RN, *et al.* (2007): Consensus nomenclature for in vivo imaging of reversibly binding radioligands. *J Cereb Blood Flow Metab* 27:1533–1539.
22. Ichise M, Toyama H, Innis RB, Carson RE (2002): Strategies to improve neuroreceptor parameter estimation by linear regression analysis. *J Cereb Blood Flow Metab* 22:1271–1281.
23. Ichise M, Liow JS, Lu JQ, Takano A, Model K, Toyama H, *et al.* (2003): Linearized reference tissue parametric imaging methods: application to [^{11}C]DASB positron emission tomography studies of the serotonin transporter in human brain. *J Cereb Blood Flow Metab* 23:1096–1112.
24. Schou M, Halldin C, Pike VW, Mozley PD, Dobson D, Innis RB, *et al.* (2005): Post-mortem human brain autoradiography of the norepinephrine transporter using (S,S)-[18F]FMeNER-D2. *Eur Neuropsychopharmacol* 15:517–520.
25. Vitiello B, Abikoff HB, Chuang SZ, Kollins SH, McCracken JT, Riddle MA, *et al.* (2007): Effectiveness of methylphenidate in the 10-month continuation phase of the Preschoolers with Attention-Deficit/Hyperactivity Disorder Treatment Study (PATS). *J Child Adolesc Psychopharmacol* 17:593–604.
26. Spencer T, Biederman J, Wilens T, Doyle R, Surman C, Prince J, *et al.* (2005): A large, double-blind, randomized clinical trial of methylphenidate in the treatment of adults with attention-deficit/hyperactivity disorder. *Biol Psychiatry* 57:456–463.
27. Meyer JH, Wilson AA, Ginovart N, Goulding V, Hussey D, Hood K, *et al.* (2001): Occupancy of serotonin transporters by paroxetine and citalopram during treatment of depression: A [^{11}C]DASB PET imaging study. *Am J Psychiatry* 158:1843–1849.
28. Kapur S (1998): A new framework for investigating antipsychotic action in humans: lessons from PET imaging. *Mol Psychiatry* 3:135–140.
29. Pacholczyk T, Blakely RD, Amara SG (1991): Expression cloning of a cocaine- and antidepressant-sensitive human noradrenaline transporter. *Nature* 350:350–354.
30. Moron JA, Brockington A, Wise RA, Rocha BA, Hope BT (2002): Dopamine uptake through the norepinephrine transporter in brain regions with low levels of the dopamine transporter: Evidence from knock-out mouse lines. *J Neurosci* 22:389–395.
31. Balcioglu A, Ren JQ, McCarthy D, Spencer TJ, Biederman J, Bhide PG (2009): Plasma and brain concentrations of oral therapeutic doses of methylphenidate and their impact on brain monoamine content in mice. *Neuropharmacology* 57:687–693.
32. Ghose S, Fujita M, Morrison P, Uhl G, Murphy DL, Mozley PD, *et al.* (2005): Specific in vitro binding of (S,S)-[3H]MeNER to norepinephrine transporters. *Synapse* 56:100–104.
33. Logan J, Ding YS, Lin KS, Pareto D, Fowler J, Biegon A (2005): Modeling and analysis of PET studies with norepinephrine transporter ligands: The search for a reference region. *Nucl Med Biol* 32:531–542.
34. Ding YS, Lin KS, Logan J (2006): PET imaging of norepinephrine transporters [review]. *Curr Pharm Des* 12:3831–3845.
35. Seneca N, Gulyas B, Varrone A, Schou M, Airaksinen A, Tauscher J, *et al.* (2006): Atomoxetine occupies the norepinephrine transporter in a dose-dependent fashion: A PET study in nonhuman primate brain using (S,S)-[,18F]FMeNER-D2. *Psychopharmacology (Berl)* 188:119–127.
36. Solanto MV (1998): Neuropsychopharmacological mechanisms of stimulant drug action in attention-deficit hyperactivity disorder: A review and integration. *Behav Brain Res* 94:127–152.
37. Volkow ND, Fowler JS, Wang GJ, Telang F, Logan J, Wong C, *et al.* (2008): Methylphenidate decreased the amount of glucose needed by the brain to perform a cognitive task. *PLoS ONE* 3:e2017.
38. Li C-SR, Huang C, Constable RT, Sinha R (2006): Imaging response inhibition in a stop signal task—neural correlates independent of signal monitoring and post-response processing. *J Neurosci* 26:186–192.
39. Ivanov I, Bansal R, Hao X, Zhu H, Kellendonk C, Miller L, *et al.* (2010): Morphological abnormalities of the thalamus in youths with attention deficit hyperactivity disorder. *Am J Psychiatry* 167:397–408.